Visible and ultraviolet Raman scattering studies of $Si_{1-x}Ge_x$ alloys

M. Holtz[a)]
Department of Physics, Texas Tech University, Lubbock, Texas 79409-1051

W. M. Duncan
Digital Imaging Technology Development, Texas Instruments, Inc., Plano, Texas 75021

S. Zollner and R. Liu
Motorola SPS, Process and Materials Characterization Laboratory, MSL, MD M360, 2200 West Broadway, Mesa, Arizona 85202

(Received 16 March 2000; accepted for publication 6 June 2000)

We report Raman studies of the Si–Si phonon band in $Si_{1-x}Ge_x$ alloys, where the excitation is by visible and ultraviolet (351 nm) light. At a wavelength 351 nm, the optical penetration depth is extremely shallow (≈5 nm). By varying the excitation from 351 to 514 nm, the optical penetration depth spans from 5 to 300 nm. Two sets of samples were examined. Thin layers grown using molecular beam epitaxy were coherently strained to match the lattice constant of the silicon substrate. Thick layers grown using organo–metallic chemical vapor deposition were strain relaxed. For the thin, strained layers, visible excitation produces a spectrum, which is a superposition of the substrate and the epilayer phonon bands. Reducing the wavelength (and, consequently, penetration depth) allows us to isolate the epilayer spectrum. Phonon energies obtained using all excitation wavelengths agree. We conclude that Raman scattering from these alloys using 351 nm laser light gives us bulk alloy properties pertinent to the near-surface composition and strain. The epilayers show no evidence of compositional variance or strain relaxation near the surface. © *2000 American Institute of Physics.* [S0021-8979(00)10317-2]

I. INTRODUCTION

Semiconductor alloys composed of silicon and germanium, $Si_{1-x}Ge_x$, where x is the germanium mole fraction, can be grown epitaxially on silicon using a variety of techniques.[1] These alloys have a bandgap which is smaller than that of pure silicon and varies with composition. The smaller bandgap also allows heavier doping without sacrificing current gain in heterojunction bipolar transistors (HBTs).[2,3] This heavy doping diminishes resistance and permits higher switching speeds. Consequently, epitaxially deposited layers of $Si_{1-x}Ge_x$ are currently gaining practical importance due to their use as graded-band gap base materials in HBTs. An important consideration in the growth of $Si_{1-x}Ge_x$ alloys on silicon substrates is strain. Since pure germanium has a lattice constant ≈4% larger than that of silicon, thin epitaxial alloy layers will be under biaxial compressive strain. If layers are grown exceeding a certain critical thickness, the strain relaxes by producing line dislocations.[4] The latter are deleterious to device performance.

Raman scattering is a proven method for examining strain and alloying properties in $Si_{1-x}Ge_x$ alloys and epilayers,[5–13] and has been recently reviewed by Liu and Cave.[14] Three vibrations are observable. The Si–Si band shows a characteristic redshift with increasing Ge dilution. The Ge–Ge band blueshifts with increasing x. The Si–Ge vibration energies exhibit only weak composition dependence. Strain shifts the phonon bands, according to

$$\omega = \omega_0 + \frac{1}{2\omega_0}[p\varepsilon_{zz} + q(\varepsilon_{xx} + \varepsilon_{yy})], \tag{1}$$

for growth on a (001) surface.[15] Here, ω_0 is the unstrained phonon energy, which depends on the alloy composition x, $\varepsilon_{xx} = \varepsilon_{yy}$ is the in-plane strain, ε_{zz} is the response strain in the growth direction, and p and q are phenomenological constants. ε_{xx} is related to the lattice parameters by the definition,

$$\varepsilon_{xx} = \varepsilon_{\parallel} = \frac{a_{\mathrm{Si}} - a(x)}{a(x)}, \tag{2}$$

where a_{Si} is the silicon substrate lattice constant, and $a(x)$ is the lattice constant of the unstrained alloy of composition x.[16,12] For $Si_{1-x}Ge_x$ grown on silicon, ε_{xx} is negative. ε_{zz} is related to ε_{xx} according to

$$\varepsilon_{zz} = -\frac{2C_{12}(x)}{C_{11}(x)}\varepsilon_{xx}, \tag{3}$$

where $C_{ij}(x)$ are the elastic stiffness constants of the $Si_{1-x}Ge_x$ alloy. Following Ref. 14, we rewrite Eq. (1) in the condensed form,

$$\omega = \omega_0 + B\varepsilon_{\parallel}, \tag{4}$$

where ω_0 is the x-dependent Si–Si phonon energy of the unstrained alloy, B is a phenomenological parameter which depends on the elastic constants, ω_0, and the Raman factors p and q. Through Eqs. (1) or (4) and knowledge of the parameters, Raman measurements permit the direct assessment of the presence of strain in an epitaxial layer.

a)Electronic mail: Mark.Holtz@ttu.edu

TABLE I. Sample growth method, composition, and thickness. The composition was determined from an average of XPS, AES, and RBS.

Growth method	x in $Si_{1-x}Ge_x$	Thickness (nm)
OMCVD	0.04	1000
	0.078	1000
MBE	0.027	116
	0.047	124
	0.069	111
	0.100	82
	0.146	87
	0.182	78
	0.224	55

In this article, we report on Raman measurements of $Si_{1-x}Ge_x$ alloys. Raman scattering is generated using 351 nm ultraviolet (UV) laser light. UV light in this photon-energy range has a very shallow optical penetration depth. In pure silicon, direct E_1 optical transitions above 3.4 eV result in a very small penetration depth. At $h\nu = 3.53$ eV ($\lambda \approx 351$ nm), $d_{opt} \equiv 1/2\alpha \approx 5$ nm in silicon, where α is the optical absorption coefficient.[17] This depth sensitivity rivals that of accepted *surface* techniques. Thus, nondestructive UV Raman has the potential of providing microstructural details from an extremely shallow, near-surface region. This approach has already been applied to obtain images of near-surface stress in patterned silicon wafers.[18] We directly compare Raman measurements of $Si_{1-x}Ge_x$ alloys, with varying composition, using several excitation wavelengths in the visible and UV. We also examined strain-relaxed alloys to isolate the effect of alloying on the phonon energies. We focus here on the Si–Si (longitudinal-optic) band, which is most intense in the composition range studied. The Si–Si phonon energy also has the strongest composition dependence of the phonon bands, permitting the most precise determination of the influence of strain. Following experimental details, we present and discuss the results of the Raman measurements. We compare the results for a given alloy composition as excitation wavelength is varied, and the effect of the composition on the Si–Si phonon band. We then summarize our results.

II. EXPERIMENTAL DETAILS

Two sets of $Si_{1-x}Ge_x$ alloys, both grown on Si (001) substrates, were studied (Table I). Samples grown by organo–metallic chemical vapor deposition (OMCVD) were thick ($\approx 1-2$ μm) and fully relaxed, as verified by x-ray diffraction. The samples grown using molecular-beam epitaxy (MBE) were coherently strained to the substrate lattice parameter.[19] The growth temperature was 550 °C for the MBE films. Compositions were determined using x-ray photoelectron spectroscopy (XPS), Rutherford backscattering (RBS), and Auger electron spectroscopy (AES). These measurements provided composition values for each sample, which were all within $\pm 1\%$ of the measurement average (Table I). Optical constants were measured using spectroscopic ellipsometry.[17] Optical constants of the alloys were determined using the methods described in Ref. 20.

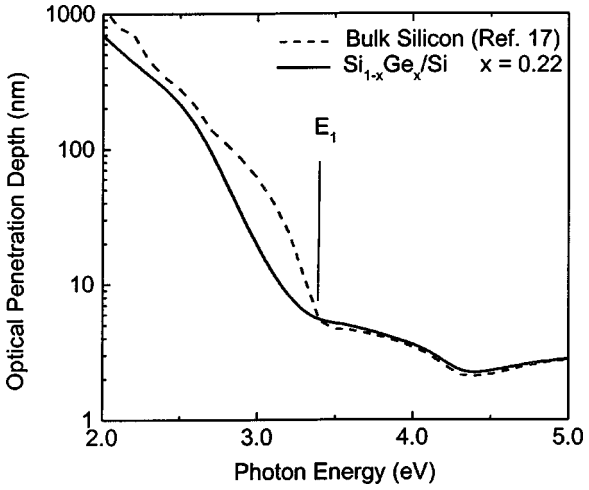

FIG. 1. Optical penetration depth ($d_{opt} = 1/2\alpha$) in MBE-grown $Si_{1-x}Ge_x$ alloy ($x = 0.22$) obtained from spectroscopic ellipsometry.

Raman measurements were carried out at room temperature. For the silicon-rich alloys studied here, the optical penetration depths are between those of the bulk silicon and germanium. A near-Brewster angle backscattering geometry was employed for the Raman measurements. Raman scatter was collected and focused into the spectrometer using UV-transmitting optical components. A 0.78 m double spectrometer was used to disperse the light. We calibrated the wavelength using known emission lines from mercury, krypton, and neon discharge lamps, and plasma lines from the lasers. A charge-coupled device detector was used to measure the spectra. Exposure times ranged from tens of seconds to several minutes.

III. EFFECT OF PHOTON ENERGY

Figure 1 shows the optical penetration depth of light into $Si_{0.78}Ge_{0.22}$, coherently strained on Si(001), versus wavelength. This spectrum was obtained using spectroscopic ellipsometry. Below 400 nm, the wavelength range of primary interest to us, light probes the epilayer with negligible penetration into the substrate. Table II lists the excitation wavelengths used in our Raman measurements, along with the corresponding optical penetration depths at those wavelengths, for pure silicon and germanium,[17] as well as for the $x = 22\%$ alloy from Fig. 1. The most important point to be extracted from Table II, and our samples thicknesses, is that the UV light used to excite our Raman spectra probes only

TABLE II. Raman excitation wavelengths used, the corresponding photon energies, and optical penetration depths into pure silicon and germanium. The last column gives d_{opt} in the MBE-grown alloy with the highest Ge composition studied.

λ (nm)	$h\nu$ (eV)	d_{opt} in Si (nm)[a]	d_{opt} in Ge (nm)[a]	$d$opt in $Si_{0.78}Ge_{.22}$
514.5	2.41	340	8	300
457.9	2.79	140	8	65
413.1	3.00	61	7	12
351.0	3.53	5	5	5

[a]Reference 17.

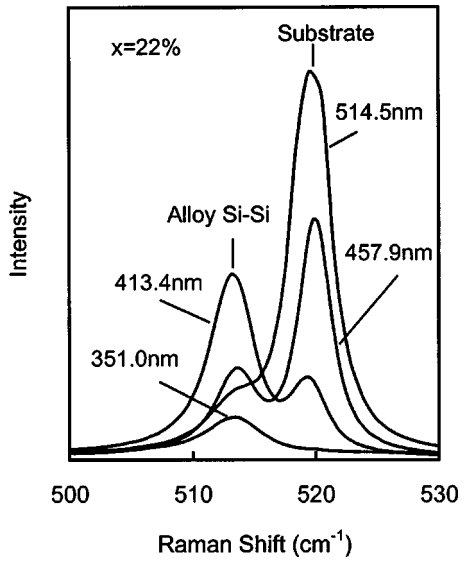

FIG. 2. Room temperature Raman spectra for an MBE-grown $Si_{1-x}Ge_x$ alloy ($x=0.22$) in the silicon fundamental vibrational energy range at several excitation wavelengths. Phonons are seen from both the alloy epilayer and the silicon substrate. At 351 nm, only the epilayer band is detected.

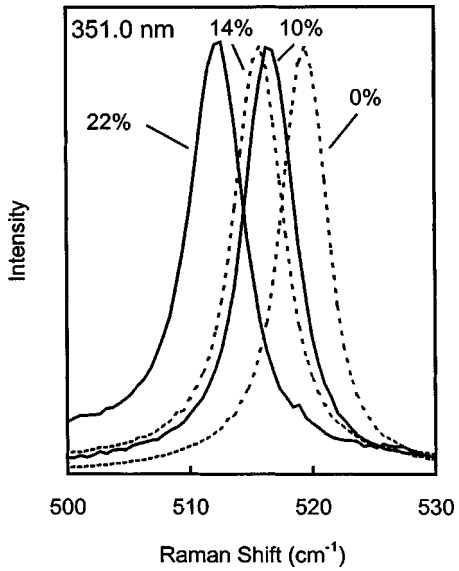

FIG. 3. Raman spectra of the excited by 351 nm light for various MBE-grown epilayers. Values of x in $Si_{1-x}Ge_x$ are noted as percents. 0% and 14% are dashed, 10% and 22% are solid traces. Intensities have been normalized for clarity. The characteristic systematic redshift is observed with increasing x.

the near-surface $Si_{1-x}Ge_x$ alloy layers. In contrast, the visible excitation will also produce scattering in the substrates of the MBE-grown samples.

Figure 2 exhibits spectra in the Si–Si phonon energy range obtained from the MBE-grown sample with $x=22\%$. Four excitation wavelengths are shown. The optic phonon $O(\Gamma)$ of pure silicon has an energy of 520 cm^{-1}. The corresponding alloy Si–Si phonon is seen near 513 cm^{-1}. The effect of alloying and strain on this phonon energy will be discussed. Intensities are normalized to that of bulk silicon at each excitation wavelength.

Clearly illustrated in Fig. 2 is the effect of optical penetration depth on the measured superposition of phonons from the substrate and epilayer. The spectrum obtained using 514.5 nm light is dominated by the substrate band at 520 cm^{-1} with only a shoulder from the alloy. The superposition limits the usefulness of Raman scattering, with excitation in this commonly used wavelength range, to thicker layers (less scattering from substrate), or layers having high germanium composition (larger phonon redshift). Since thin, coherently strained alloys with $x \leqslant 25\%$ are desired in HBT applications, alloy composition, and strain determination are more precisely obtained using Raman scattering excited by laser lines having shorter wavelengths, as follows. As the wavelength (and probe depth) are varied into the deep blue (457.9 nm) and near UV (413.1 nm) in Fig. 2 the intensity emphasis shifts from being dominated by the substrate band to that of the epilayer. At 351.0 nm only the epilayer band is observed, with no scattering seen from the substrate. The variation in relative intensities is well described using a simple scattering-volume calculation, in which

$$I_{\text{alloy}} \propto \int_0^t e^{-2\alpha_{\text{alloy}}x}dx = \frac{1}{2\alpha_{\text{alloy}}}(1-e^{-2\alpha_{\text{alloy}}t}) \tag{5}$$

and

$$I_{\text{substrate}} \propto e^{-2\alpha_{\text{alloy}}t}\int_t^\infty e^{-2\alpha_{\text{substrate}}x}dx$$

$$= \frac{1}{2\alpha_{\text{substrate}}}e^{-2\alpha_{\text{alloy}}t}e^{-2\alpha_{\text{substrate}}t}. \tag{6}$$

Here, the intensities are assumed to be in direct proportion to the scattering volumes of the epilayer (thickness t) and substrate, respectively. This ignores other factors, which may vary with wavelength, such as the Raman scattering cross section. By calculating the relative intensities ($I_{\text{substrate}}/I_{\text{alloy}}$) using Eqs. (5) and (6) and comparing these with the measured intensities (Fig. 2), we obtain the expected direct dependence. Agreement between the epilayer phonon energies and linewidths, over the excitation wavelength range in Fig. 2, demonstrates the ability to probe extremely thin layers of $Si_{1-x}Ge_x$ alloys (or silicon) using UV generated Raman scattering. The generally good agreement between alloy phonon energies obtained with visible and UV excitations show that we probe bulk alloy properties, rather than surface-related effects. This argument is substantiated by measurements of samples with other compositions, to be discussed.

IV. COMPOSITION DEPENDENCE OF THE RAMAN SPECTRA

Figure 3 shows Raman spectra varying x with a 351 nm excitation wavelength. Each of these samples was grown using MBE, and is fully strained. The linewidth does not change with alloy composition, showing that the epilayers are highly commensurate with the substrate across the full composition range studied. With a 351 nm excitation, each alloy exhibited only phonon bands from the epilayer with no substrate spectrum. The spectra in Fig. 3 show the consistent redshift of the Si–Si phonon energy with increasing composition, as has been reported in the literature.[7,8] Intensities of

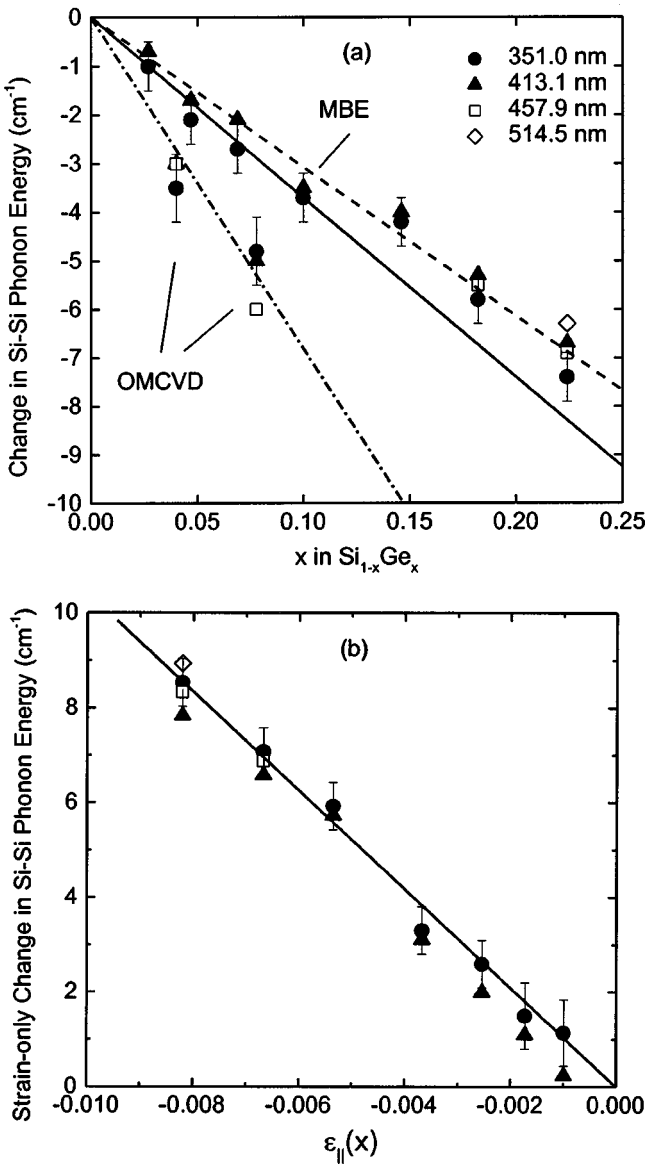

FIG. 4. (a) Summary data of the shift in the Si–Si phonon energy, from that of bulk silicon, versus x. Data designated as OMCVD samples corresponds to strain-relaxed epilayers. The trend is due to alloying effects only (dashed-dot line). All other data points are for the fully strained MBE epilayers. The dashed line is a linear fit to the latter data. The solid line is from Eqs. (1)–(3). (b) Summary data of the shift of the Si–Si phonon energy for the MBE-grown films with the effect of alloying subtracted using Eq. (7). Error bars are shown for the 351 nm data only; they are representative of each data set.

the Si–Si band were found to generally decrease with increasing x, although there was scatter in the intensity data. (Data in Fig. 3 are rescaled to have approximately the same amplitude.) The intensity reduction can be attributed to the reduced silicon concentration,[21] variations in the absorption coefficient, and gradual shifting of the direct energy transition (E_1) away from near resonance with the 351 nm excitation.

Figure 4 summarizes Raman data obtained for all samples listed in Table I. Shown in Fig. 4(a) is the composition-dependent shift in energy of the Si–Si phonon from the $O(\Gamma)$ energy (520 cm^{-1}) in bulk silicon. Data are extracted from measurements using those wavelengths for which the epilayer Si–Si feature was intense enough to meaningfully deconvolute from the substrate band. This became increasingly difficult at lower germanium compositions, except when using the 351 nm excitation, which showed no substrate band. Results from the two OMCVD samples (strain relaxed) show a strong redshift with increasing germanium concentration. Data for the various excitation wavelengths are in good accord. The dash-dot line has a slope of -68 cm^{-1} taken from Refs. 9 and 12. This line corresponds to fully strain-relaxed $Si_{1-x}Ge_x$ alloys and describes the effect of alloying only. Good agreement is seen between the dashed line (obtained across a wider composition range) and our measurements. Thus,

$$\omega_0(x) = 520.0 - 68x \tag{7}$$

describes the composition dependent unstrained phonon energy (cm^{-1}) in Eqs. (1) or (4).[9,12]

We now turn our attention to the results from the fully strained MBE samples. The dashed line in Fig. 4(a) is a linear fit to these data points, with a slope $d\omega_{\mathrm{meas}}/dx = -30.7 \pm 0.6\,\mathrm{cm}^{-1}$. This slope is the combined result of alloying and strain. The quantity $d\omega_{\mathrm{meas}}/dx$ varies between literature accounts. Our value is at the lower end (absolute value) among the range of reported values, and is qualitatively described by the combined effects of strain and alloying. Using Vegard's law to obtain elastic constants,[22] and constants p and q for Si from Ref. 25 and Eqs. (1)–(3) give a linear slope of -37 cm^{-1} in the $x < 0.25$ range. This analysis results in the expected blueshift due to substrate-induced, biaxial compressive strain in the alloy epilayer. The net result, strain plus alloying, is shown as the solid line in Fig. 4(a). The agreement between the data and the calculated trend agrees well in the low x range, but shows a discrepancy at higher x. One possible explanation for the difference between the observed and calculated trends at high x may be the very large strains present in our samples. This translates into an enormous stress, beyond the regime obtainable in the uniaxial stress studies used to determine p and q.[25] Nonlinear elastic theory may be needed to adequately describe the effects of extremely large stress (strain) on phonon energies. Furthermore, the use of parameters p and q from measurements of bulk silicon (for the Si–Si vibration) may not be correct. Evidence that the p and q parameters of the alloys differ from those of bulk silicon can be extracted from the hydrostatic pressure investigations of Sui, Burke, and Herman.[23] They find that the mode-Grüneisen parameter,

$$\gamma = B_0 \frac{\partial \ln \omega}{\partial P} = \frac{1}{6\omega_0^2}(p + 2q), \tag{8}$$

varies strongly with alloy composition, increasing from 1.0 at $x = 0$ to 1.2 at $x = 0.25$ for the Si–Si mode. Here, B_0 is the bulk modulus, a function of x. Since γ is related to p and q the increase observed in the hydrostatic pressure measurements may be due in part to changes in p and q of the alloys. However, because p and q combine differently to make up B and γ, it is difficult to attribute the observed B_{meas} to changes in one parameter or the other. These preliminary notions require further investigations. It would be desirable to include data from the Ge–Ge mode, and possibly the Si–Si and

TABLE III. Collection of literature values of the rate at which the Si–Si phonon shifts with x in $Si_{1-x}Ge_x$, together with reported values of B in Eq. (4).

Reference	B_{mean} (cm^{-1})
7	−600
13	−863
12	−962 (at $x=0.3$)
5	−940
8	−931
27	−930
14	−1008
This work	-1040 ± 23

Ge–Ge transverse-acoustic modes, as part of further analysis, to address the large number of parameters encountered here.

Figure 4(b) shows the strain-only shift in the Si–Si phonon energy, obtained by plotting $\omega-\omega_0(x)$, vs $\varepsilon_{\parallel}(x)$. Data are well described by a linear fit with slope $B_{meas}=-1040\pm23\,cm^{-1}$. The literature values of B_{meas} collected in Table III show a spread in the values determined for B_{meas}, with our result having the largest magnitude and in good agreement with what is reported by Liu and Cave.[14] According to their analysis, a lower value of B_{meas} implies a reduced strain in the epilayer, by an amount $\delta\varepsilon$. Thus, Eq. (4) must be recast as

$$\omega-\omega_0(x)=B(\varepsilon_{\parallel}(x)-\delta\varepsilon)=B_{meas}\varepsilon_{\parallel}(x) \tag{9}$$

with

$$B_{meas}=B\left(1-\frac{\delta\varepsilon}{\varepsilon_{\parallel}(x)}\right). \tag{10}$$

Since $B_{meas}<B$, the reduced strain results in a smaller shift in the phonon energy according to Eq. (9).

The most likely causes of strain relaxation in $Si_{1-x}Ge_x$/Si epilayers would be line dislocations formed during growth or postgrowth cooling.[24] As the thickness of an epilayer increases, it approaches the composition-dependent critical thickness (h_c) for strain relaxation.[4] We suggest that *partial* relaxation is achieved by introducing line dislocations sufficient in areal density to reduce the strain energy and leave the average alloy at nonzero strain. Thus, the critical thickness should benchmark a range of thicknesses. Films having a thickness just below h_c will have a tendency to partially relax, with the density of dislocations increasing with thickness until, well above h_c, full strain relaxation occurs. Larger values of B_{meas} thus correspond to a higher degree of pseudomorphic strain. Definitively determining B is an elusive task, since there will always be some degree of strain relaxation. Within this interpretation, our value of B_{meas} gives the lowest strain relaxation reported. Lockwood and Baribeau[12] have pointed out that B_{meas} varies with excitation wavelength, with the general trend being a reduction with smaller wavelength. Because shorter wavelengths will probe shallower regions, diminished B_{meas} values have been plausibly attributed to relaxation of the near-surface strain.[25] We do not see significant deviation in the data corresponding to different wavelengths in Fig. 4, which include data obtained with UV excitation (very shallow optical penetration depth). We also do not see variation in the line width of the Si–Si phonon with excitation wavelength. From these two observations, the simplest conclusion is that the composition of our samples is uniform along the growth direction, and that there is no evidence of near-surface strain relaxation in our samples. The depth range of validity for this conclusion is from ≈5 nm to the full thickness of the layer, bearing in mind that we measure an average property over the optical penetration depth for a given laser line. The assertion that the composition is uniform throughout the growth layer is supported by RBS depth-profiling measurements of the MBE-grown layers.[26,27] These show a 1%–2% composition deviation over the full thickness of the epilayer, supporting the Raman-based notion that the composition is uniform (within experimental uncertainties) in these films.

V. CONCLUSIONS

We have measured the Raman spectra of $Si_{1-x}Ge_x$ alloys using 351 nm excitation. This light probes a very shallow, near-surface region. We directly compare these results with those obtained using standard visible Raman spectroscopy (Fig. 2). We conclude that the UV probe provides information about the *bulk* alloy properties even though it is the near-surface (≈5 nm) composition and strain environment being examined. No evidence of strain relaxation at the surface is obtained. The trend observed in the Si–Si phonon energy of the strain relaxed epilayers shows varied degrees of agreement with previous measurements performed using visible excitation. Most notably, the slope observed in the strain-only Raman shift versus strain ($-1040\pm23\,cm^{-1}$), has a magnitude at the high end of reported values. This is interpreted as evidence that very little strain relaxation is present in our MBE films.[14] The Raman method thus suggests itself as a means by which strain can be measured for a set of deposition conditions. Varying the wavelength into the UV, as we have done here, is found to be a method by which information on near-surface stress relaxation (or stress depth profiling) can be assessed.

ACKNOWLEDGMENTS

One of the authors (M.H.) wishes to acknowledge grants from Texas Instruments and the State of Texas Advanced Technology Program in support of this work. The authors thank Glen Wilks for the alloy growth.

[1] J. C. Bean, in *Semiconductors and Semimetals-Germanium Silicon: Physics and Materials*, edited by R. K. Willardson and E. R. Weber (R. Hull and J. C. Bean, Vol. eds.) (Academic, San Diego, 1999), Vol. 56, p. 1.
[2] U. Konig, *IEEE Colloquium Advances in Semiconductor Devices* (IEEE, London, 1999), p. 6.
[3] D. J. Paul, Adv. Mater. **11**, 191 (1999).
[4] R. Hull, in *Semiconductors and Semimetals-Germanium Silicon: Physics and Materials*, edited by R. K. Willardson and E. R. Weber (R. Hull and J. C. Bean, Vol. eds.) (Academic, San Diego, 1999), Vol. 56, p. 102.
[5] B. Dietrich, E. Bugiel, J. Klatt, G. Lippert, T. Morgenstern, H. J. Osten, and P. Zaumseil, J. Appl. Phys. **74**, 3177 (1993).
[6] Z. M. Jiang *et al.*, Appl. Phys. Lett. **75**, 370 (1999).
[7] F. Cerdeira, A. Pinczuk, J. C. Bean, B. Batlogg, and B. A. Wilson, Appl. Phys. Lett. **45**, 1138 (1984).

[8] F. Lu, C. H. Perry, F. Namavar, N. L. Rowell, and R. A. Soref, Appl. Phys. Lett. **63**, 1243 (1993).
[9] M. I. Alonso and K. Winer, Phys. Rev. B **39**, 10056 (1989).
[10] M. Franz, K. F. Dombrowski, H. Rücker, B. Dietrich, K. Pressel, A. Barz, U. Kerat, P. Dold, and K. W. Benz, Phys. Rev. B **59**, 10614 (1999).
[11] P. M. Mooney, F. H. Dacol, J. C. Tsang, and J. O. Chu, Appl. Phys. Lett. **62**, 2069 (1993).
[12] D. J. Lockwood and J.-M. Baribeau, Phys. Rev. B **45**, 8565 (1992).
[13] J. C. Tsang, P. M. Mooney, F. H. Dacol, and J. O. Chu, J. Appl. Phys. **75**, 8098 (1994).
[14] R. Liu and N. Cave, in *SiGeC Alloys and their Applications*, edited by S. T. Pantelides and S. Zollner (Gordon and Breach, New York, in press).
[15] F. Cerdeira, C. J. Buchenauer, F. H. Pollak, and M. Cardona, Phys. Rev. B **5**, 580 (1972).
[16] J. P. Dismukes, L. Elstrom, and R. J. Paff, J. Phys. Chem. **10**, 3021 (1964).
[17] D. E. Aspnes and A. A. Studna, Phys. Rev. B **27**, 985 (1983).
[18] M. Holtz, J. C. Carty, and W. Duncan, Appl. Phys. Lett. **74**, 2008 (1999).
[19] J. C. Bean, L. C. Feldman, A. T. Fiory, S. Nakahara, and I. K. Robinson, J. Vac. Sci. Technol. A **2**, 436 (1984).
[20] G. E. Jellison, T. E. Haynes, and H. H. Burke, Opt. Mater. **2**, 105 (1993).
[21] Naively, the Si–Si bond probability, and hence the associated scattering intensity, will have a composition dependence which is proportional to $(1-x^2)$.
[22] S. S. Mitra and N. E. Massa, in *Handbook on Semiconductors*, edited by T. S. Moss (North-Holland, Amsterdam, 1986), Vol. 1, p. 96.
[23] Z. Sui, H. H. Burke, and I. P. Herman, Phys. Rev. B **48**, 2162 (1993).
[24] Another possible cause of strain reduction is the unintentional incorporation of small impurities during deposition.
[25] E. Anastassakis, A. Cantarero, and M. Cardona, Phys. Rev. B **41**, 7529 (1990).
[26] J. Keenan (unpublished).
[27] M. A. G. Halliwell, M. H. Lyons, S. T. Davey, M. Hockly, C. G. Tuppen, and C. J. Gibbings, Semicond. Sci. Technol. **4**, 10 (1989).